S1 ChronoLoess database

S1.1 Selection of luminescence data

For the chronological modelling, we pooled luminescence ages from 77 publications reporting chronologies for 93 loess records from 16 loess regions from all over Europe. We provide the entire dataset of the extracted data as a supplement for inspection. The inspected publications reported more than 1500 ages thereof we extracted 1,423 single luminescence ages from quartz, feldspar or polymineral fractions. While some isolated recommendations exist on reporting luminescence data (e.g., Duller 2008; Bateman 2019), those are seldomly followed and, to date, the luminescence-dating community has not agreed on data-reporting standards. Similar, software tools used to analyse data and calculate ages often remain unreported (for a discussion, see Kreutzer et al., 2017). This situation puts up a barrier that severely impedes the recycling and comparison of luminescence age records and is further complicated by the number of single parameters to consider for the age calculation (e.g., Zink 2013). Unfortunately, there is no simple way to circumnavigate this issue and tap into the otherwise excellent and unique chronological datasets covering mainly the Late Pleistocene.

We followed a five-step strategy to minimise the errors during the data extraction. (1) Luminescence data of interest were extracted manually from original papers and supplementary data by Mathieu Bosq and Sebastian Kreutzer, creating one XLS file per loess area (randomly assigned). (2) Sebastian Kreutzer validated all single XLS-sheets cross-checking information with the original studies and complemented data that were missing or erroneously assigned, and (3) compiled one master XLS sheet with all data. (4) The master XLS file was further used for spotting errors and removing inconsistency.

In order to use the published luminescence data in our chronological modelling, we made a couple of processing decisions we outline in the following.
1. We did not use published ages but extracted numerical quantities published along the ages such as radio-nuclide concentrations or equivalent doses, compiled them in *MS Excel^{TM}* tables, and recalculated the ages with the dose rate and age calculator *DRAC* (v.1.2, Durcan et al., 2015). This decision allowed us to cancel out systematic deviations between datasets resulting from, e.g., age calculation software tools applied dose-rate conversion factors.
2. We treated most datasets reporting IRSL (this includes post-IR IRSL data) as minimum ages to avoid incorporating potential systematic errors from fading corrections (cf. King et al., 2018) and measurements of the fading rate itself (cf. public preprint discussion Kadereit et al., 2020). Higher signal stability was reported for ages derived from post-IR IRSL at 290 ˚C measurements (e.g., Buylaert et al., 2012), and studies often assume negligible fading or reported inclusive results that allows the authors to circumvent a fading correction. Residual doses, so far reported, were not subtracted. We refer the reader to the supplement for full details of selected and discarded datasets.
3. We applied a couple of decisions to the calculations themselves. Namely, we recalculated all cosmic and environmental dose rates using *DRAC*; external Rb was always calculated from potassium. In rare cases, the original study did not report sufficient information but provided only processed data for, e.g., cosmic dose rates and environmental dose rates and the data could not be recalculated.
4. Except for rare cases of apparent mistakes (for instance, typos), other parameters combined with high numbers of degrees of freedom (e.g., alpha-efficiency, internal dose-rates, measurement protocol parameters, statistical data treatment) were always taken as reported by the study's authors. Missing or faulty units and citations were not considered an error if the data appeared meaningful.

In other words, we placed wagers on the authors' knowledge and insight, making expert decisions on individual parameters, which includes fundamental decisions such as the chosen mineral and grain size fraction or the method to estimate radionuclide concentrations.
The original study (including the supplement) did not support sufficient information to recalculate the luminescence ages in sporadic cases. Such results were considered non-reproducible and marked as discarded. For the following list of parameter selections, we refer to **Table S1**.

Naturally, our selection remains imperfect without accessing and reanalysing raw data. However, such data are usually not available. Hence, we believe that our approach provides the best possible compromise about data available, and the amount of data likely leads to average effects with extreme values, providing sufficient statistical confidence in the modelling results.

Table S1: Overview of the *DRAC* parameter decisions applied for age recalculation. The template for this table was taken from the DRAC user guide (https://www.aber.ac.uk/en/dges/research/quaternary/luminescence-research-laboratory/dose-rate-calculator/?show=userguide).

COLUMN	PARAMETER	SELECTION AND REMARKS
TI:1	Project ID	Arbitrary naming
TI:2	Sample ID	ID as published in the original study, partly combined with information on protocol or mineral
TI:3	Mineral	"Q" for quartz, "F" for feldspar or "PM" for polymineral
TI:4	Conversion factors	"Liritzisetal2013" for conversion after Liritz et al. (2013)
TI:5	External U (ppm)	Values, as reported in the original study. If activity instead of values instead of concentration values were reported, the values were recalculated with the function calc_Activity2Concentration() from the R package 'Luminescence' (Kreutzer et al., 2012, 2020). In the case of radioactive disequilibria, we followed the advice of the original study.
TI:6	External δU (ppm)	
TI:7	External Th (ppm)	
TI:8	External δTh (ppm)	
TI:9	External K (%)	
TI:10	External δK (%)	
TI:11	External Rb (ppm)	
TI:12	External δRb (ppm)	
TI:13	Calculate external Rb from K conc?	Chosen option for all datasets, "Y", means that the external Rb was calculated from the potassium concentration after Mejdahl (1987).
TI:14	Internal U (ppm)	Internal nuclide concentrations were applied as reported by the original study.
TI:15	Internal δU (ppm)	
TI:16	Internal Th (ppm)	
TI:17	Internal δTh (ppm)	
TI:18	Internal K (%)	
TI:19	Internal δK (%)	
TI:20	Internal Rb (ppm)	
TI:21	Internal δRb (ppm)	
TI:22	Calculate internal Rb from K conc?	No internal Rb was calculated from the internal K concentration.
TI:23	User external $\dot{D}\alpha$ (Gy.ka^{-1})	External dose rates were set to 0 to recalculate the values from published U, Th, and K concentrations. Except for two cases: (1) No U, Th, K, but external dose-rates were

TI:24	User external δḊα (Gy.ka⁻¹)	published by the original study and (2) external gamma-dose rates measured *in situ*. We calculated dry dose rates using published water content values because *DRAC* inputs dry dose rates. However, this was only possible if contemporary measured water contents from the samples were reported.
TI:25	User external Ḋβ (Gy.ka⁻¹)	
TI:26	User external δḊβ (Gy.ka⁻¹)	
TI:27	User external Ḋγ (Gy.ka⁻¹)	
TI:28	User external δḊγ (Gy.ka⁻¹)	
TI:29	User internal Ḋr (Gy.ka⁻¹)	Internal dose rates were taken from the original study. If the study quoted internal nuclide concentrations instead, those values were applied, and the parameter set to 0.
TI:30	User internal δḊr (Gy.ka⁻¹)	
TI:31	Scale Ḋγ at shallow depths?	The parameter was set to "N" for all datasets, i.e., the gamma-dose rate was not scaled for shallow depths.
TI:32	Grain size min (µm)	Grain sizes were inserted as reported in the original study.
TI:33	Grain size max (µm)	
TI:34	α-Grain size attenuation factors	We applied the setting "Brennanetal1991" to all datasets to calculate alpha-dose grain-size attenuations, according to Brennen et al. (1991).
TI:35	β-Grain size attenuation factors	We applied the setting "Guerinetal2012-Q" to quartz samples and "Guerinetal2012-F" to feldspar and polymineral samples to use grain-size related attenuation factors for the beta-dose after Guérin et al. (2012)
TI:36	Etch depth min (µm)	If the study reported etching with HF and assumed that the alpha-affected outer rim of a grain was removed, we applied 18 µm as minimum etch depth and 22 µm as maximum etch depth. If the original study made diverting assumptions for *DRAC,* these values were used.
TI:37	Etch depth max (µm)	
TI:38	β-Etch attenuation factor	We consistently applied the setting "Brennan2003" to all datasets to use beta-etch attenuation factors after Brennan (2003).
TI:39	a-value	We applied values as reported by the original study. In sum studies, nothing was mentioned, in such a case, we applied standard literature values, such as 0.035 ± 0.003 for quartz (Lai et al., 2008).
TI:40	δa-value	
TI:41	Water content (%)	We applied values as reported by the original study. However, few studies reported the water content without uncertainty. To avoid this precision bias becoming too large compared to other studies, we applied a relative uncertainty of 20% (of the given value in %) to all those studies.
TI:42	δWater content (%)	
TI:43	Depth (m)	Values were taken as reported in the original study. A few studies did not report the sample depth needed to calculate the cosmic dose rate. We estimated the sample depth for these samples based on drawings and information provided in the study.
TI:44	δDepth (m)	
TI:45	Overburden density (g.cm⁻³)	We assumed an overburden sediment density of 1.8 ± 0.2 g cm⁻³ for all datasets. However, if the original study reported a density estimate, this value was taken instead.
TI:46	δOverburden density (g.cm⁻³)	
TI:47	Latitude (decimal degrees)	Values were deduced from the original study. If nothing was reported, those values were estimated through *Google Earth^{TM}*.

TI:48	Longitude (decimal degrees)	
TI:49	Altitude (m asl)	Values were deduced from the original study. If nothing was reported, those values were estimated through *Google Earth*^{TM}.
TI:50	User-defined $\dot{D}c$ (Gy.ka^{-1})	The input was set to "X" for all datasets, i.e., cosmic dose-rate was recalculated for datasets using *DRAC*.
TI:51	User-defined $\delta\dot{D}c$ (Gy.ka^{-1})	
TI:52	De (Gy)	We inserted values as reported by the original study. Values reported as 2-sigma were recalculated and entered as 1-sigma uncertainties.
TI:53	δDe (Gy)	

S1.2 Quality control

We have extracted the original study data with the greatest care and subsequently validated it; however, such manual extraction is seldom error-free. Expected are typos or an otherwise wrong extraction of the original data due to human error. Furthermore, age differences are expected due to our re-calculation, using different correction factors or other assumptions, such as no residual correction or different statistical moments.

To estimate the data quality, we randomly sampled 100 datasets and compared the age results reported in the original study with the results recalculated using *DRAC*. Although age is an aggregated variable, it enables a fast and straightforward data inspection. Systematic errors should show in unexpected offsets, not justified by the applied parameter settings. We considered age discrepancies of 20% caused by the recalculation of the ages expected and acceptable, while higher deviations indicate input errors requiring an inspection and, if justified, a correction. We assumed that less than 5% of our datasets will contain such errors.

In 7 out 92 datasets (one turned out invalid) we found age discrepancies larger than 20% compared to the original study (**Fig. S1**). Four turned out input errors (e.g., missing radioelement input, inserting Bq instead of %) in the *DRAC* table, for the remaining three the differences seem to originate in the calculation of the original study. While it is likely that our full datasets still contain copy errors, the random selection led to the correction of similar mistakes for other samples (e.g., missing input of radioelements or wrong dimension). Hence, it is safe to assume that >95% of the entries in our dataset are free of systematic copy errors.

Published ages vs DRAC recalculation
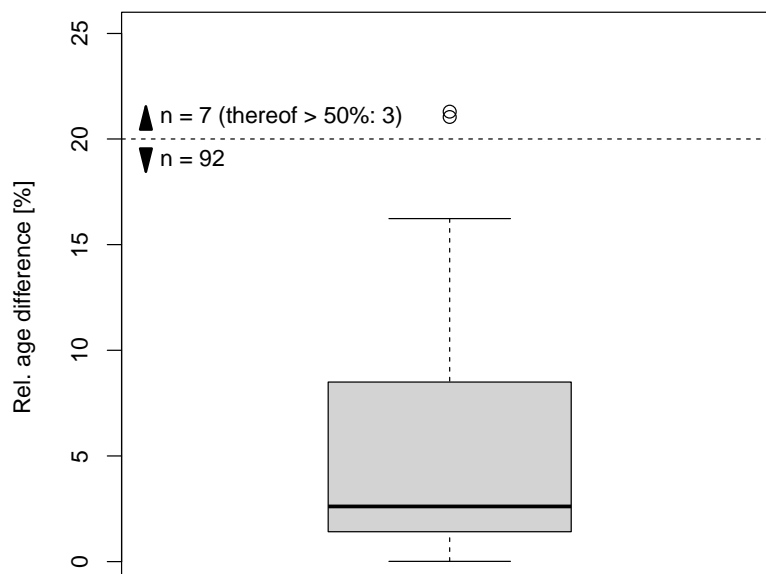
Figure S1 Relative age difference of age reported in the original study and in the *DRAC* table.

S2 Bayesian age-depth models
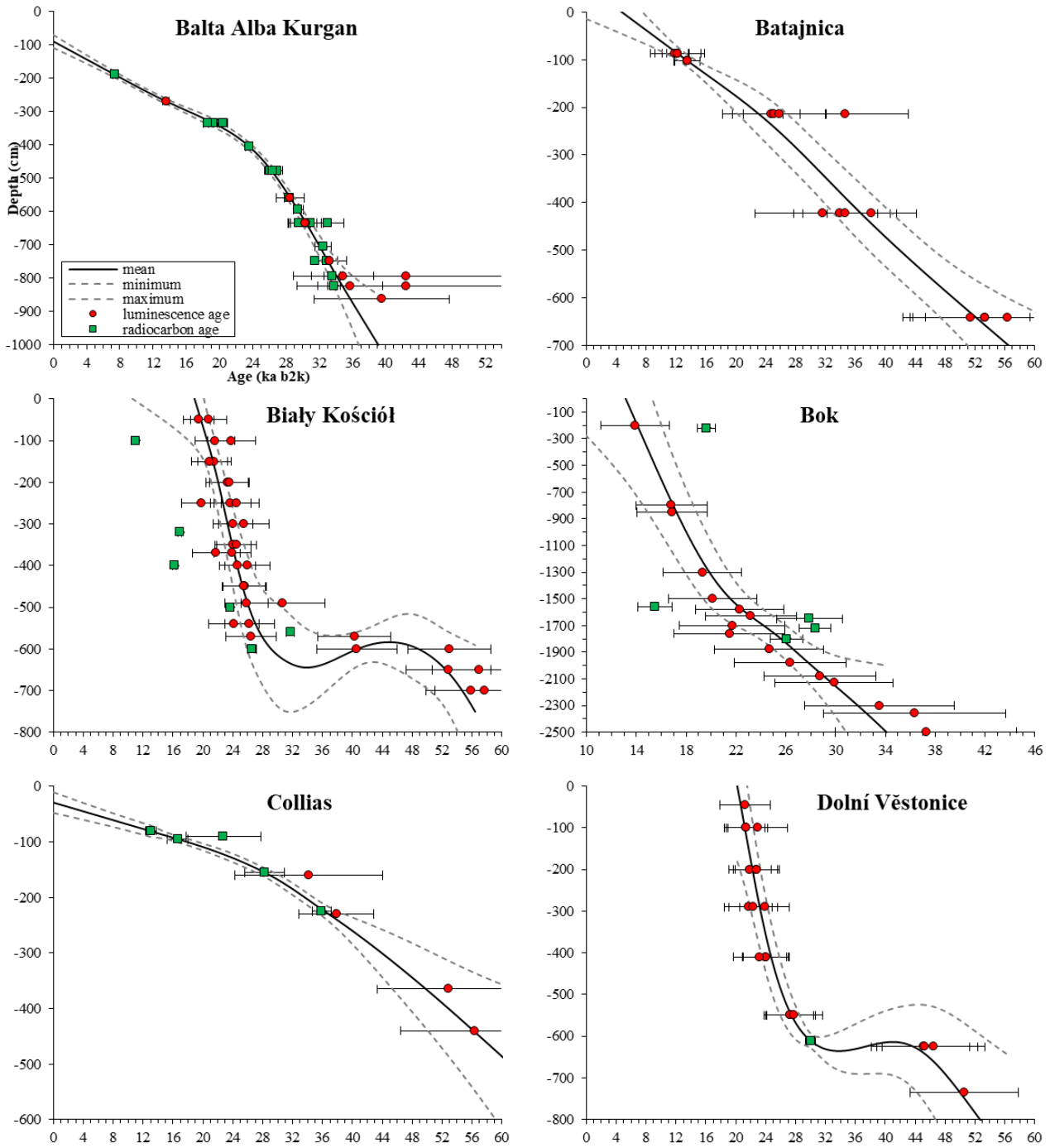
Figure S2 Bayesian age-depth model results using the ChronoModel software. The red circles and the green squares show the luminescence and radiocarbon calibrated ages respectively with their error bars (1σ). The grey lines represent the minimum and maximum age limits (95.4% probability intervals). The black line shows the mean age-depth model (continued on the next page).
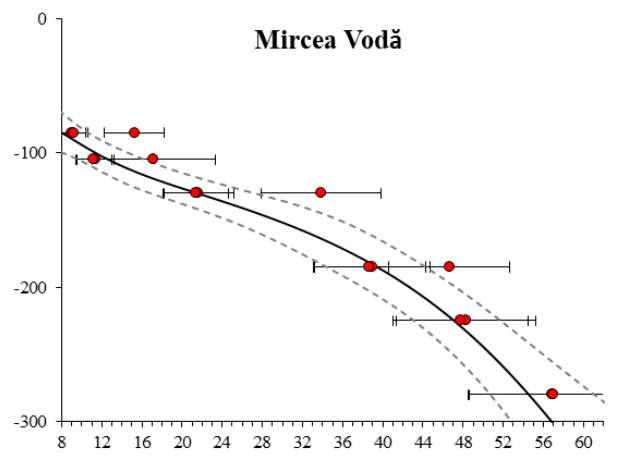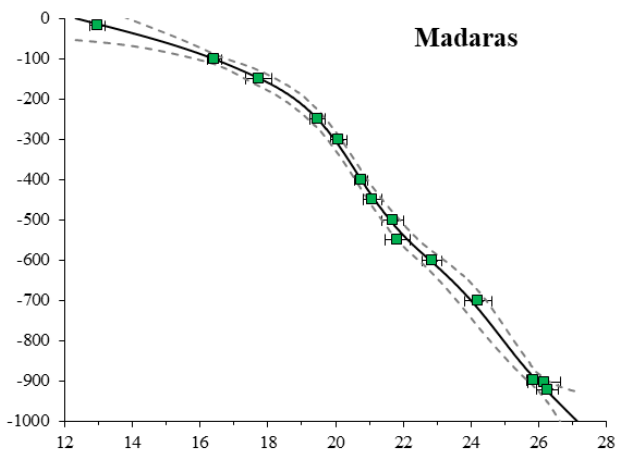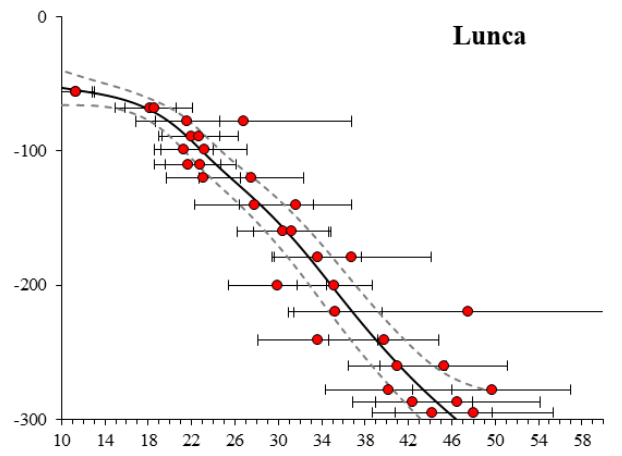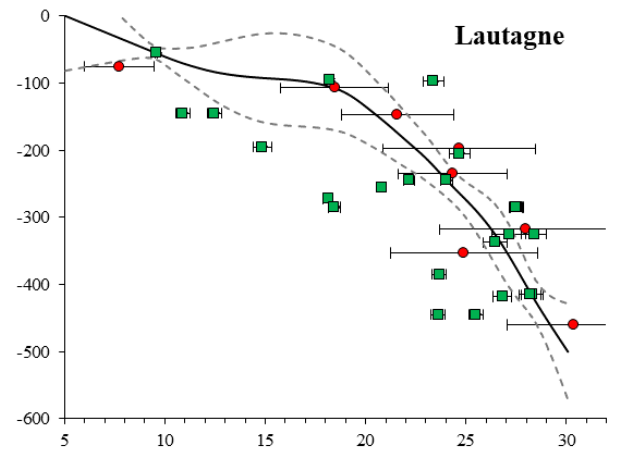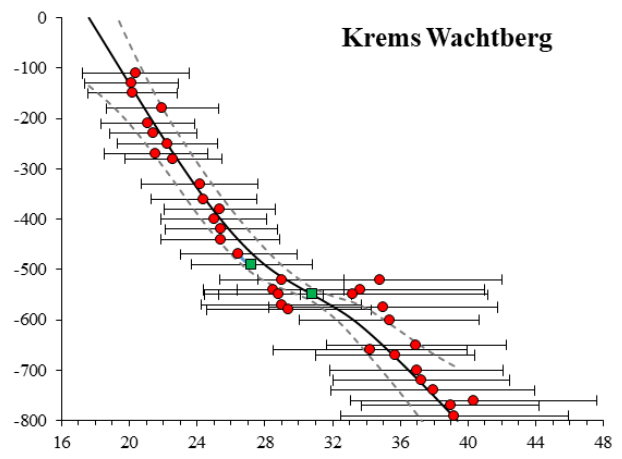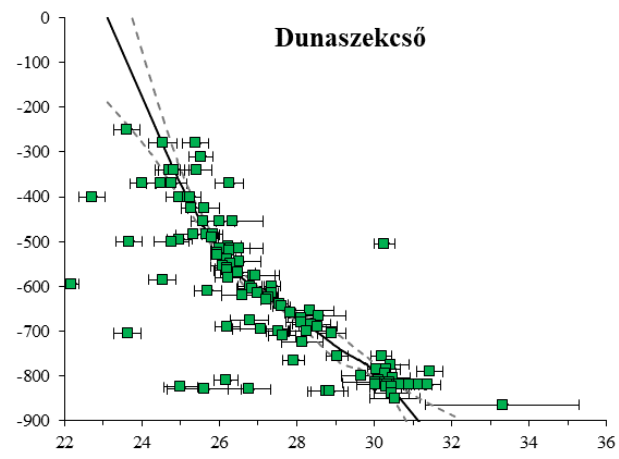
Figure S2 continued on the next page.
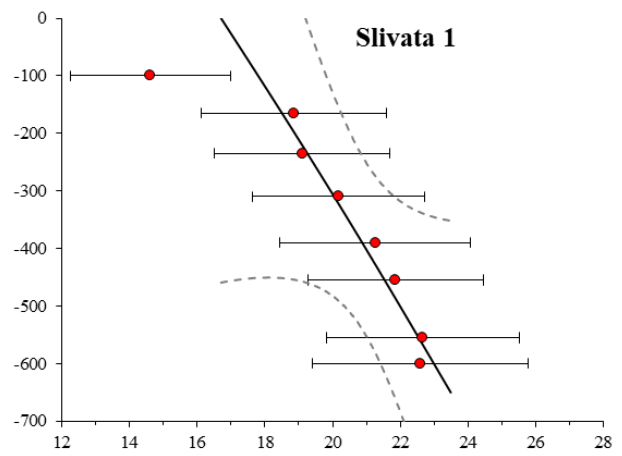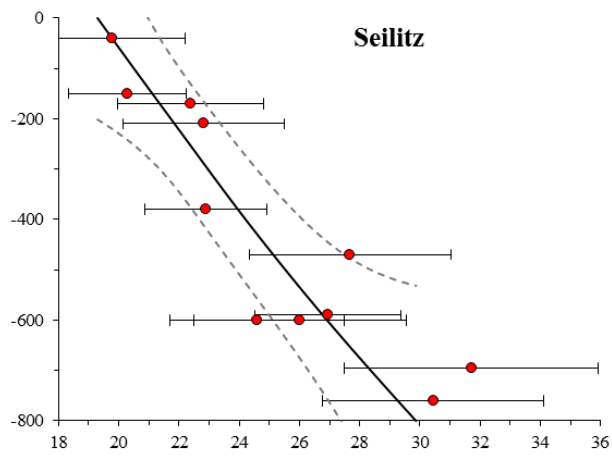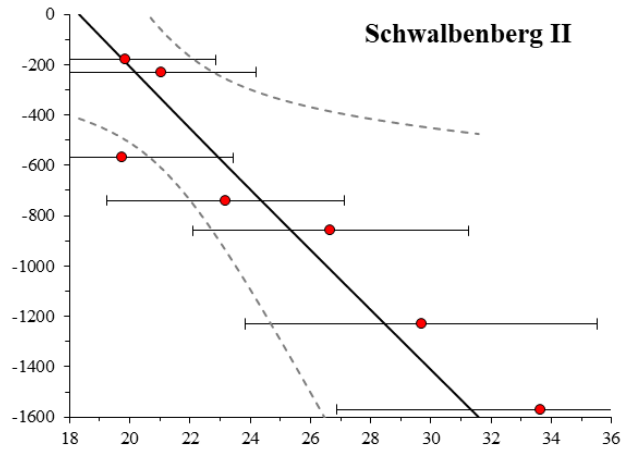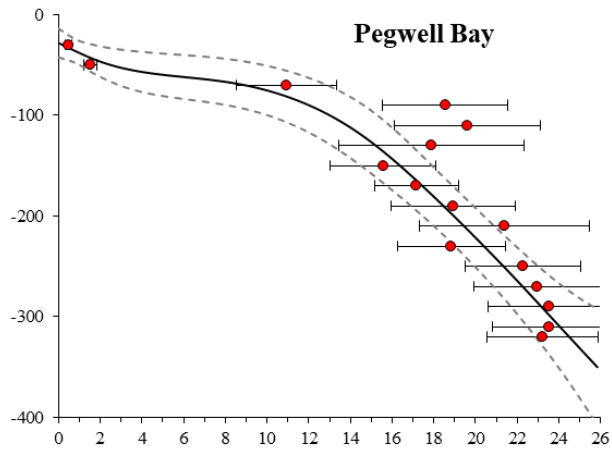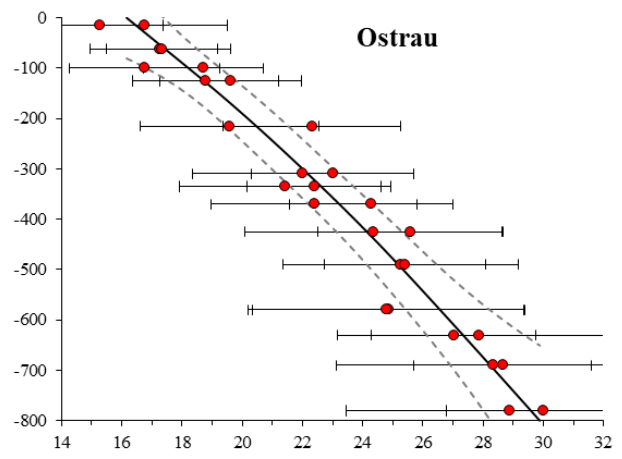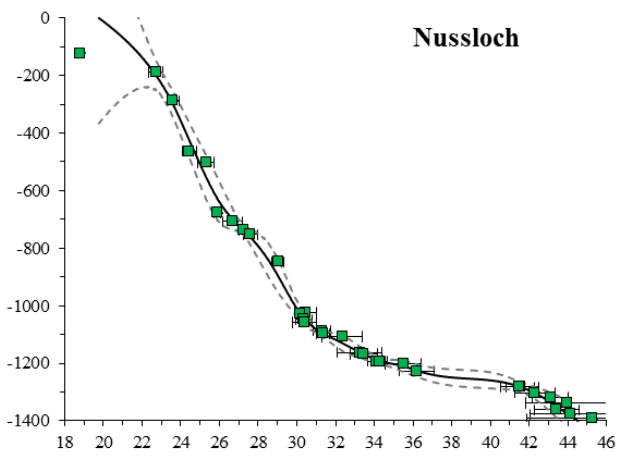
Figure S2 continued on the next page.

Figure S2 Bayesian age-depth model results using the ChronoModel software. The red circles and the green squares show the luminescence and radiocarbon calibrated ages respectively with their error bars (1σ). The grey lines represent the minimum and maximum age limits (95.4% probability intervals). The black line shows the mean age-depth model (continued on the next page).

S3 Mass Accumulation Rates
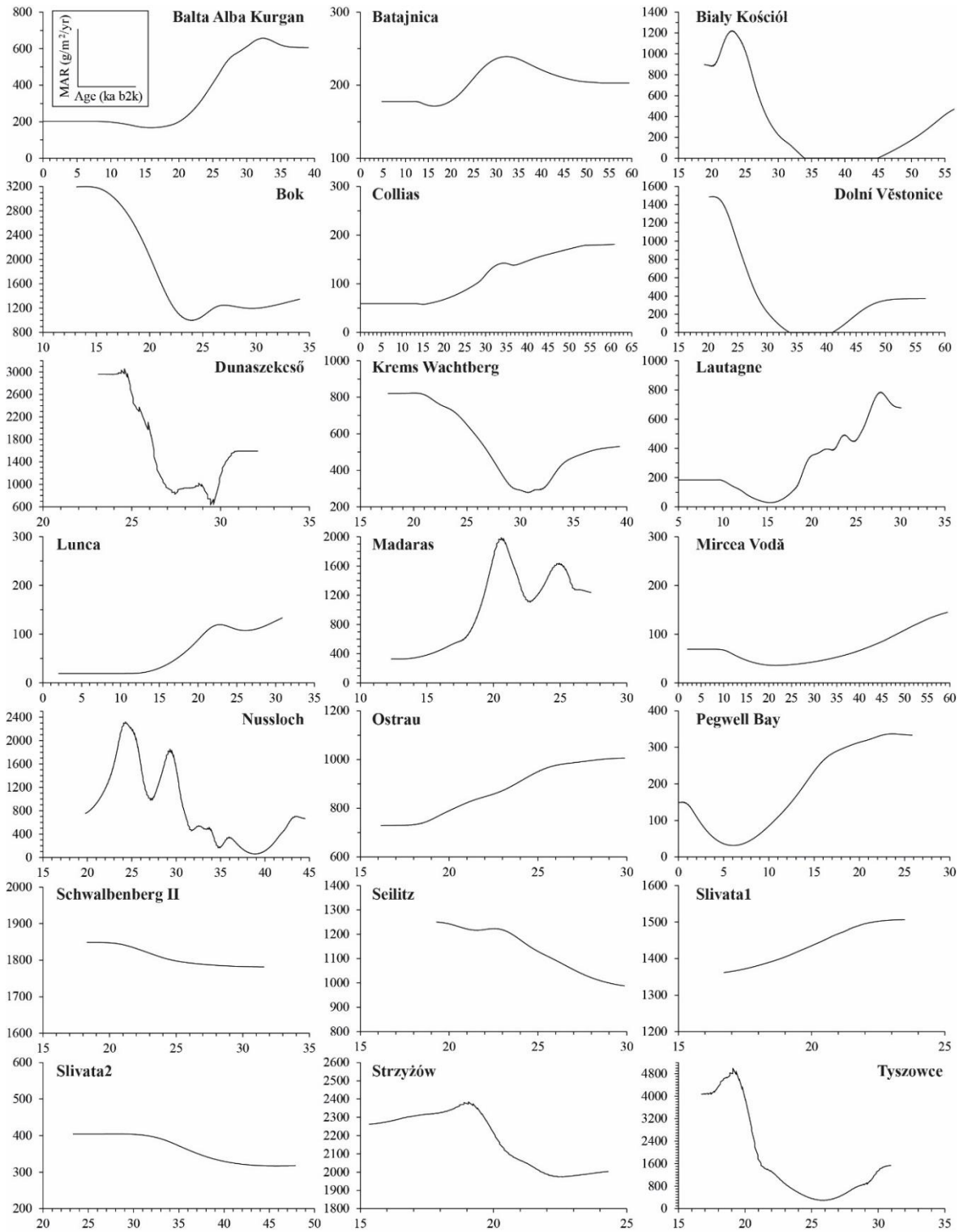
Figure S3 Mass accumulation rates (MARs) derived from age-depth model (part 1/2).
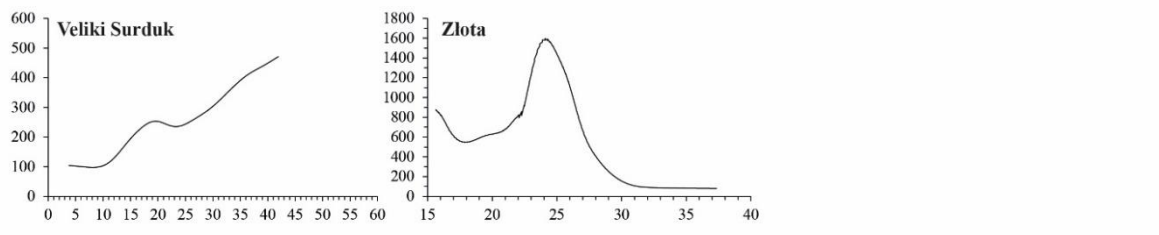
Figure S3 Mass accumulation rates (MARs) derived from age-depth model (part 2/2).

References

Bateman, M.D., 2019. Handbook of Luminescence Dating. Whittles Publishing, Dunbeath, Scotland, UK.

Brennan, B.J., Lyons, R.G., Phillips, S.W., 1991. Attenuation of alpha particle track dose for spherical grains. International Journal of Radiation Applications and Instrumentation. Part D. Nuclear Tracks and Radiation Measurements 18, 249–253. doi:10.1016/j.radmeas.2006.05.011

Brennan, B.J., 2003. Beta doses to spherical grains. Radiation Measurements 37, 299–303. doi:10.1016/S1350-4487(03)00011-8

Buylaert, J.P., Jain, M., Murray, A.S., Thomsen, K.J., Thiel, C., Sohbati, R., 2012. A robust feldspar luminescence dating method for Middle and Late Pleistocene sediments. Boreas 41, 435–451. doi:10.1111/j.1502-3885.2012.00248.x

Duller, G.A.T., 2008. Luminescence Dating: guidelines on using luminescence dating in archaeology. Swindon: English Heritage.

Durcan, J.A., King, G.E., Duller, G.A.T., 2015. DRAC: Dose Rate and Age Calculator for trapped charge dating. Quaternary Geochronology 28, 54–61. doi:10.1016/j.quageo.2015.03.012

Guérin, G., Mercier, N., Nathan, R., Adamiec, G., Lefrais, Y., 2012. On the use of the infinite matrix assumption and associated concepts: A critical review. Radiation Measurements 47, 778–785. doi:10.1016/j.radmeas.2012.04.004

Kadereit, A., Kreutzer, S., Schmidt, C., and DeWitt, R.: A closer look at IRSL SAR fading data and their implication for luminescence dating, Geochronology Discuss. [preprint], https://doi.org/10.5194/gchron-2020-3, 2020.

King, G.E., Burow, C., Roberts, H.M., Pearce, N.J.G., 2018. Age determination using feldspar: Evaluating fading-correction model performance. Radiation Measurements 119, 58–73. doi:10.1016/j.radmeas.2018.07.013

Kreutzer, S., Schmidt, C., Fuchs, M.C., Dietze, M., Fischer, M., Fuchs, M., 2012. Introducing an R package for luminescence dating analysis. Ancient TL 30, 1–8.

Kreutzer, S., Burow, C., Dietze, M., Fuchs, M.C., Schmidt, C., Fischer, M., Friedrich, J., Riedesel, R., Autzen, M., Mittelstrass, D. 2020. Luminescence: Comprehensive Luminescence Dating Data Analysis. R package version 0.9.11. https://CRAN.R-project.org/package=Luminescence

Kreutzer, S., Burow, C., Dietze, M., Fuchs, M.C., Fischer, M., Schmidt, C., 2017. Software in the context of luminescence dating: status, concepts and suggestions exemplified by the R package `Luminescence'. Ancient TL 35, 1–11.

Lai, Z., Zöller, L., Fuchs, M., Brückner, H., 2008. Alpha efficiency determination for OSL of quartz extracted from Chinese loess. Radiation Measurements 43, 767–770. doi:10.1016/j.radmeas.2008.01.022

Liritzis, I., Stamoulis, K., Papachristodoulou, C., Ioannides, K., 2013. A Re-Evaluation of Radiation Dose-Rate Conversion Factors. Mediterranean Archaeology and Archaeometry 12, 1–15.

Mejdahl, V., 1987. Internal radioactivity in quartz and feldspar grains. Ancient TL 5, 10–17.

Zink, A., 2013. A coarse Bayesian approach to evaluate luminescence ages. Geochronometria 40, 90–100. doi:10.2478/s13386-013-0105-x